journal

J. Am. Ceram. Soc., **87** [4] 670–76 (2004)

Distribution of Grain Boundaries in $SrTiO_3$ as a Function of Five Macroscopic Parameters

David M. Saylor*

National Institute of Standards and Technology, Gaithersburg, Maryland 20899

Bassem El Dasher,† Tomoko Sano,* and Gregory S. Rohrer*

Department of Materials Science and Engineering, Carnegie Mellon University, Pittsburgh, Pennsylvania 15213-3890

Measurements of the grain boundary population as a function of misorientation and boundary plane orientation show that the distribution is inversely correlated to the sum of the energies of the surfaces comprising each boundary. The observed correlation suggests that the difference between the energy of a high-angle grain boundary and the two component surfaces is relatively constant as a function of misorientation. Two exceptions to this correlation were identified: low-misorientation-angle boundaries and the coherent twin boundary, where the (111) planes in the adjoining crystals are parallel to each other, but rotated by 60° around the [111] axis. In these cases, the high degree of coincidence across this interface probably lowers the boundary energy with respect to that of the component surfaces. For all other boundaries, the anisotropy of the population is accurately predicted by the surface energy anisotropy, and in general, boundaries display a preference for {100} orientations, the planes of minimum surface energy.

I. Introduction

To distinguish one type of grain boundary from another at the mesoscale, the values of five independent parameters must be specified. Three parameters describe the lattice misorientation and two parameters describe the interface normal. The number of distinct combinations of these parameters is so large that it has been common practice to simplify the situation by studying variations in the population and properties over only a subset of the variables.[1] For example, some studies measure only the distribution of misorientations while others concentrate on special orientation relationships, such as high coincidence configurations. By taking advantage of automated digital microscopy, it is now possible to measure the relative frequency of occurrence of a grain boundary as a function of both misorientation and boundary plane normal.

The work described here was motivated by two interesting observations that resulted from a five-parameter analysis of grain boundaries in MgO.[2] The first observation is that there are preferred orientations for grain boundary planes and the population distribution exhibits an inverse correlation with the grain boundary energy. In other words, the most frequently observed boundaries have the lowest energies. The second and more surprising observation is that the variations in the energies of general boundaries correlate to a model based on the sum of the free surface energies of the constituent planes. If we imagine creating a grain boundary by first creating the two free surfaces and then joining them, we can say that the boundary energy is the sum of the two surface energies, minus a binding energy that results from the interactions of the atoms on either side of the interface.[3] The observed correlation between the grain boundary and surface energies indicates that this binding energy is approximately constant for different boundaries. While special cases with remarkable planar coincidence are expected to have significantly increased binding energies (for example, low-angle boundaries), it is a reasonable hypothesis for general boundaries where the superimposed repeat units on either side of the boundary are incommensurate.

The most appealing feature of the correlation between surface energy, grain boundary energy, and population is that the surface energy is only a two-parameter function and, in comparison to the five-parameter grain boundary energy, is more easily measured. Therefore, if the correlation between these quantities proves to be a general trend in polycrystalline materials, then it has the potential to greatly accelerate our understanding of grain boundary anisotropy. The purpose of this paper is to test the generality of the observations in MgO by measuring the distribution of grain boundaries in $SrTiO_3$ and determining the extent of its correlation to the surface energy anisotropy.

II. Experimental Procedure

The grain boundary distribution, $\lambda(\Delta g,\mathbf{n})$, is defined as the relative frequency of occurrence of a unit area of grain boundary with misorientation, Δg, and boundary plane normal, $\mathbf{n}$. The distribution is measured in units of multiples of a random distribution (MRD) so that if the distribution of grain boundaries were random, then the value of λ at all values of Δg and $\mathbf{n}$ would be 1. The value of λ is greater than 1 when the total area of a specific type of boundary is larger than would be expected in a random distribution; values less than 1 are associated with the types of boundaries whose total areas are less than expected in a random distribution. The methods used to measure $\lambda(\Delta g,\mathbf{n})$ for $SrTiO_3$ are similar to those used in the study of MgO; a detailed account of these methods has already been published.[4] The aspects of the experimental procedure that differ from the earlier reports are described below.

Because the polycrystalline sample used for the current study was previously used to measure the surface energy anisotropy, its preparation has already been described in detail.[5] Of relevance to the current paper, the sample was made from 99% pure $SrTiO_3$ ($Pm\bar{3}m$) powder (Aldrich Chemical Co., Inc., Milwaukee, WI)[6] and the final heat treatment was a 1650°C anneal in air for 20 h. After this step, the grain size was ~90 μm. The sample was then lapped flat with a 3 μm alumina slurry to remove the surface region and polished with a 0.02 μm colloidal silica slurry to create

J. E. Blendell—contributing editor

Manuscript No. 10408. Received July 21, 2003; approved November 24, 2003.
This work was supported by the MRSEC program of the National Science Foundation under Award No. DMR-0079996.
*Member, American Ceramic Society.
†Current address: University of California, Lawrence Livermore National Laboratory, P.O. Box 808, Livermore, California 94511.

a surface that was flat to within ± 0.2 μm over the entire sample surface. To reveal the positions of the grain boundaries, the polished sample was thermally etched at 1400°C for 6 min in air. Grain boundary migration was not observed during this final procedure. It should be noted that while the grooves were formed at 1400°C, the grain boundary configurations were determined by the high-temperature anneal at 1650°C and results reported here are representative of grain boundaries in the bulk of the sample at this temperature.

The grain boundary configurations were determined by analyzing data from two parallel planar sections, each with an area of 0.3 cm^2, but vertically separated from each other by 5.2 ± 0.3 μm. Each section was characterized using arrays of many smaller overlapping orientation imaging microscopy (OIM) and optical microscopy images. The positions of the grain boundaries were derived from the optical images and the misorientations across the boundaries were determined from the OIM images. A portion of these data are illustrated in Fig. 1. More than 5000 distinct grains were identified and more than 1×10^5 triangular segments or individual boundary planes were used to approximate the continuous interfacial network. We estimate that of these planar segments, there are at least 3×10^4 distinct boundaries that are sometimes subdivided in smaller segments.

To classify each triangular segment, we specify the misorientation (Δg) using three Eulerian angles (ϕ_1, Φ, ϕ_2) and the boundary plane orientation (**n**) using two spherical angles (θ, ϕ). These angles are parameterized by ϕ_1, $\cos\Phi$, ϕ_2, $\cos\theta$, and ϕ, so that the domain can be easily partitioned into equal volume units. Here, each range of $\pi/2$ is divided into nine discrete cells, so that the continuous function $\lambda(\Delta g,\mathbf{n})$ is approximated by a discrete set of grain boundary types. This is easiest to understand by visualizing the misorientation domain as a three-dimensional rectangular parallelepiped. This is represented schematically in Fig. 2(a), which also indicates the range of each parameter. Each point in this space corresponds to a particular misorientation, and for each point we can plot the distribution of grain boundary normals, **n**, on a two-dimensional stereographic projection in the range of $0 \le \phi \le 2\pi$ and $0 \le \cos\theta \le 1$, as illustrated in Fig. 2(b). Note that for each of the 9^3 misorientations there are $4{\cdot}9^2$ directions for **n**, and this yields a total of $4{\cdot}9^5$ (=236,196) cells in the five-dimensional domain. Of these, 6561 are crystallographically distinguishable. After adding the area of each observed triangular grain boundary segment to its corresponding equivalent cells, the area in each cell is normalized by the average area per cell so that the resulting

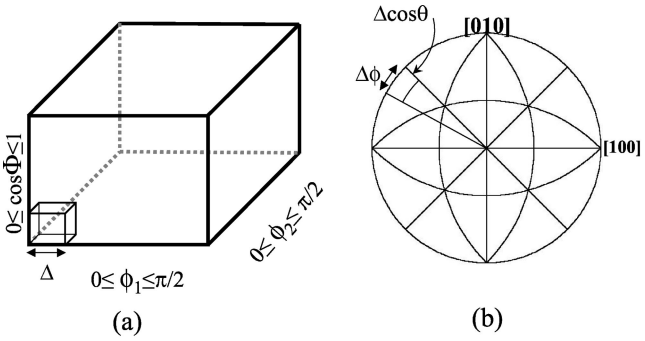

Fig. 2. Parameterization of $\lambda(\Delta g,\mathbf{n})$ into (a) three lattice misorientation parameters and (b) two boundary plane orientation parameters. In the misorientation space, there are 9^3 cells and for each of these cells, there is a stereographic projection for the boundary plane normals with $4{\cdot}9^2$ cells.

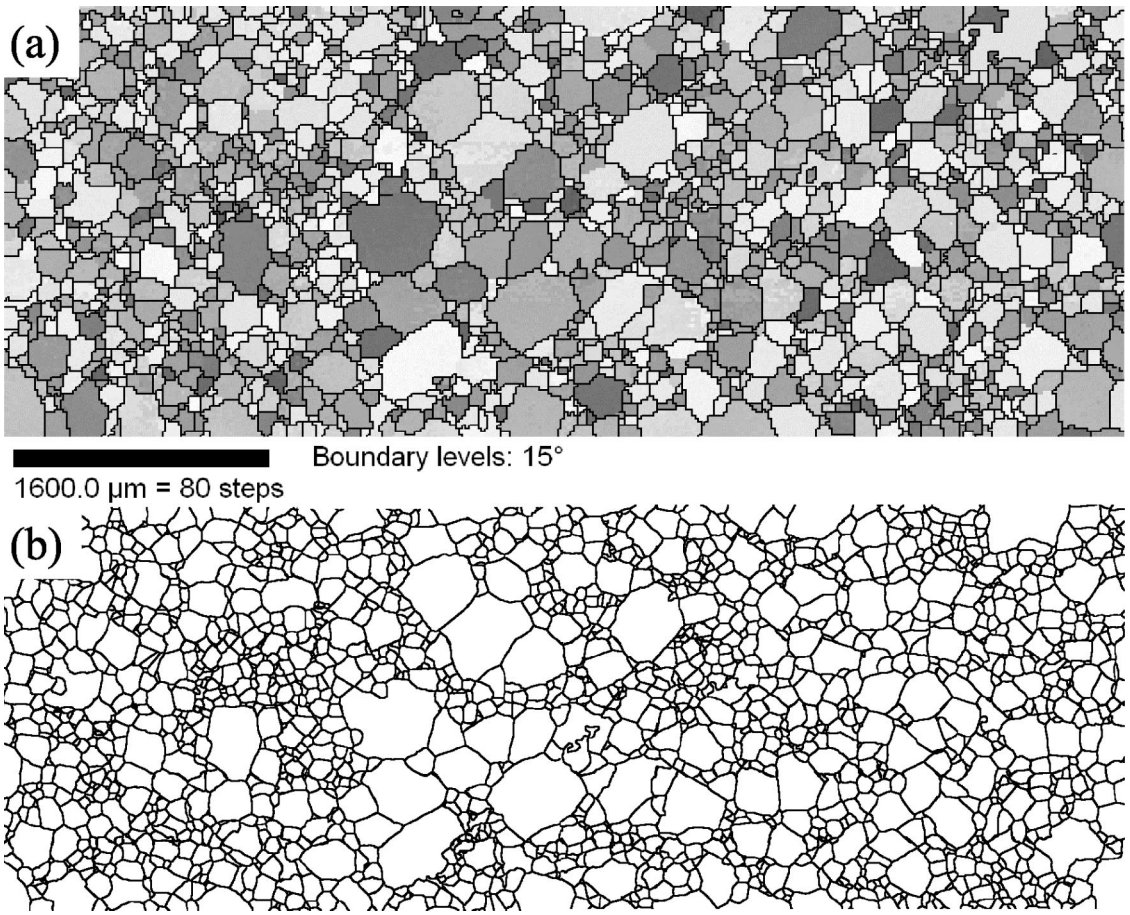

Fig. 1. (a) EBSP grain map and (b) grain boundary skeleton of the $SrTiO_3$ sample. These images show 40% of the analyzed surface area on one layer of the sample. Areas of constant gray level in the EBSP grain map have a constant orientation. For display purposes, an iterative cleanup procedure was implemented that eliminated unreliable points by dilating the grains to replace the poorly indexed data points by their correctly indexed neighbors.

value is a multiple of a random distribution (MRD). The details involved in recording and analyzing the data have been described previously.[4] In the next section, we will examine $\lambda(\mathbf{n})$ at different misorientations.

III. Results

The $SrTiO_3$ examined here had no significant grain orientation texture. The grain misorientation texture was also weak. The only prominent feature was an enhancement of the population of low-misorientation-angle grain boundaries, which peaked at a value of 2.43 MRD. In contrast to our previous study of MgO, this situation permits a more comprehensive analysis. In the prior study, the sample had strong axial ⟨111⟩ texture.[4] Because the sample was sectioned in planes perpendicular to this axis, the observed population of [111] twist boundaries, including the coherent twin ($\Sigma 3$), was artificially lower than the true population. The random texture of the $SrTiO_3$ sample makes it possible to characterize the entire range of grain boundary types.

Although the orientation and misorientation texture were limited, the grain boundary planes did show preferred orientations. The frequency of grain boundary plane normals ($\lambda(\mathbf{n})$) for all observed grain boundaries, regardless of misorientation, are shown in stereographic projection down the [001] axis in Fig. 3(a). The peaks on this plot indicate grain boundary plane orientations that make up a higher than random fraction of the entire grain boundary area and valleys indicate plane orientations that are more scarce than expected in a random distribution. In this case, grain boundaries are more frequently terminated by {100} planes than any other orientation.

Recent measurements of the surface energy anisotropy of $SrTiO_3$ have shown that the minimum occurs at the (100) orientation.[5] For comparison, this result is reproduced in Fig. 3(b). This comparison illustrates the qualitative trend that grain boundaries comprised of low-energy surfaces are observed more frequently than those made up of higher-energy surfaces. This trend is quantified in Fig. 4(a), which illustrates the correlation between the grain boundary population and the minimum angular deviation of the grain boundary plane normal from ⟨100⟩. Boundaries near ⟨100⟩ occur with twice the frequency of those that are 45° from ⟨100⟩. The correlation between the sum of the surface energies that make up the boundary and the population is shown in Fig. 4(b). This illustrates that boundary configurations made up of low-energy surfaces are observed more frequently than those made up of high-energy surfaces. To quantify this relationship, we have used the Spearman[7,8] rank-order correlation coefficient (r_s), which ranges from −1 to 1, to indicate perfect negative and positive correlations, respectively; for $r_s = 0$, no correlation exists. Using this measure, $r_s = -0.63$, which indicates a moderate to strong negative correlation.

The anisotropy in $\lambda(\mathbf{n})$ at fixed values of the misorientation parameters always varies by a factor of 2 or more and, therefore, is larger than suggested by the misorientation averaged data (Fig. 3(a)). To display the data, we choose a misorientation axis and a rotation about that axis (this corresponds to picking a point in the three-dimensional space in Fig. 2(a)) and then plot the two-dimensional distribution of grain boundary plane normals on a stereographic projection. A selection of these data is shown in Fig. 5, where the distribution of plane orientations for grain boundaries with 20° misorientations about [110], [111], and [952] are shown. Note that as indicated by the data in Figs. 3 and 4, the trend is that the distribution

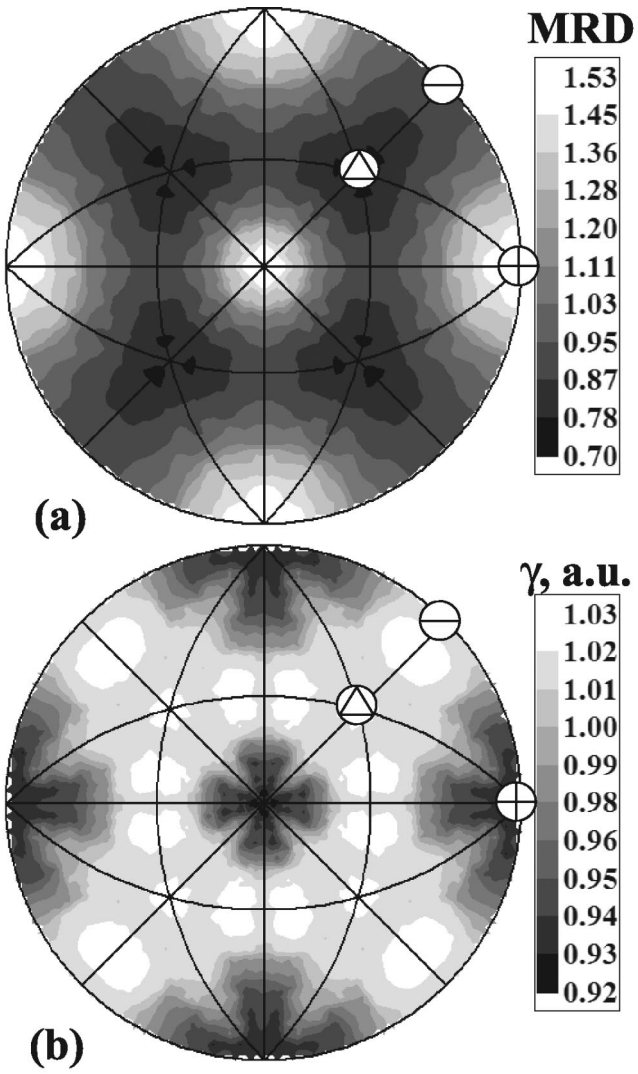

Fig. 3. (a) Misorientation averaged distribution of grain boundary planes plotted in stereographic projection. The (100), (110), and (111) planes are marked by ⊕, ⊖, and a circle with a triangle, respectively. (b) The surface energy of $SrTiO_3$ at 1400°C, also plotted in stereographic projection, from Ref. 5.

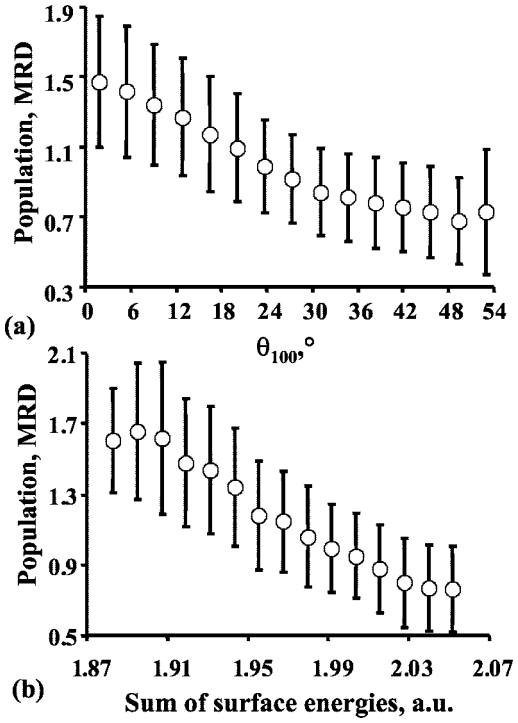

Fig. 4. (a) Values of the grain boundary population as a function of the minimum angular deviation of the two grain boundary planes from ⟨100⟩, θ_{100}. The circle at each value of θ_{100} is the average of all values within a range of 3.65°. (b) The average value of the population plotted as a function of the sum of the two surface energies. The circle at each value represents the average population for all boundaries within a range of 0.012 au; in both graphs, the bars indicate 1 standard deviation above and below the mean.

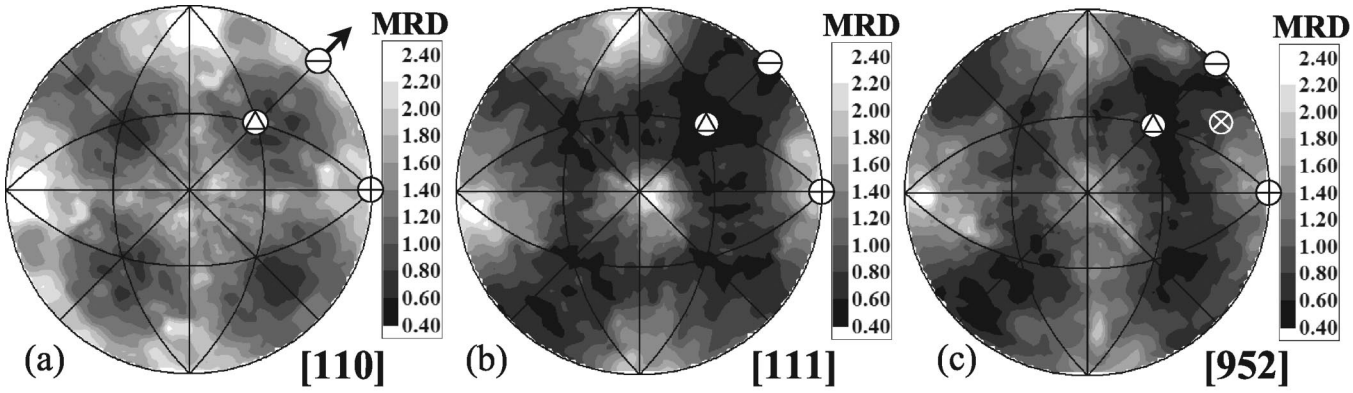

Fig. 5. Observed distribution of grain boundary plane normals for boundaries with 20° misorientations about the (a) [110], (b) [111], and (c) [952] axes. The units are in MRD and the distribution is plotted in stereographic projection. In (a), the misorientation axis lies in the plane of the page and is shown as an arrow; in (b) it is inclined with repsect to the paper at the [111] position, marked by a triangle; and in (c) it is also inclined with respect to the plane and denoted by an ×.

always peaks near {100}. To illustrate the details of the correlation between the surface energy and grain boundary population at individual misorientations, the population of grain boundary planes observed at three misorientations about [100] is compared with the hypothetical energy anisotropy constructed from the measured surface energy anisotropy (see Fig. 6). Note that for all misorientations about the [100] axis, the population peaks at the (100) position. This is the pure twist boundary (**n** is parallel to [100]) for which both sides of the boundary are terminated by a low-energy (100) plane, regardless of the misorientation angle. For other types of boundaries, if one of the two crystals is terminated by a {100} plane, then the complementary plane terminating the second crystal must be inclined by the misorientation angle away from {100}. This is clearly seen along the zone of tilt boundaries (from (010), through (001), to $(0\bar{1}0)$) for the 40° misorientation (Fig. 6(c)), where there is a peak at (001) and at a position 40° from this orientation. In fact, grain boundary configurations where one or both of the terminating planes are {100} are responsible for the vast majority of all observed peaks in the distribution, and these data illustrate the general trend that the maxima in the observed distribution correlate with the minima in the hypothetical energy.

IV. Discussion

The purpose of this research was to test the idea that the grain boundary population is correlated to the sum of the energies of the surfaces comprising the boundary. The observations reported here

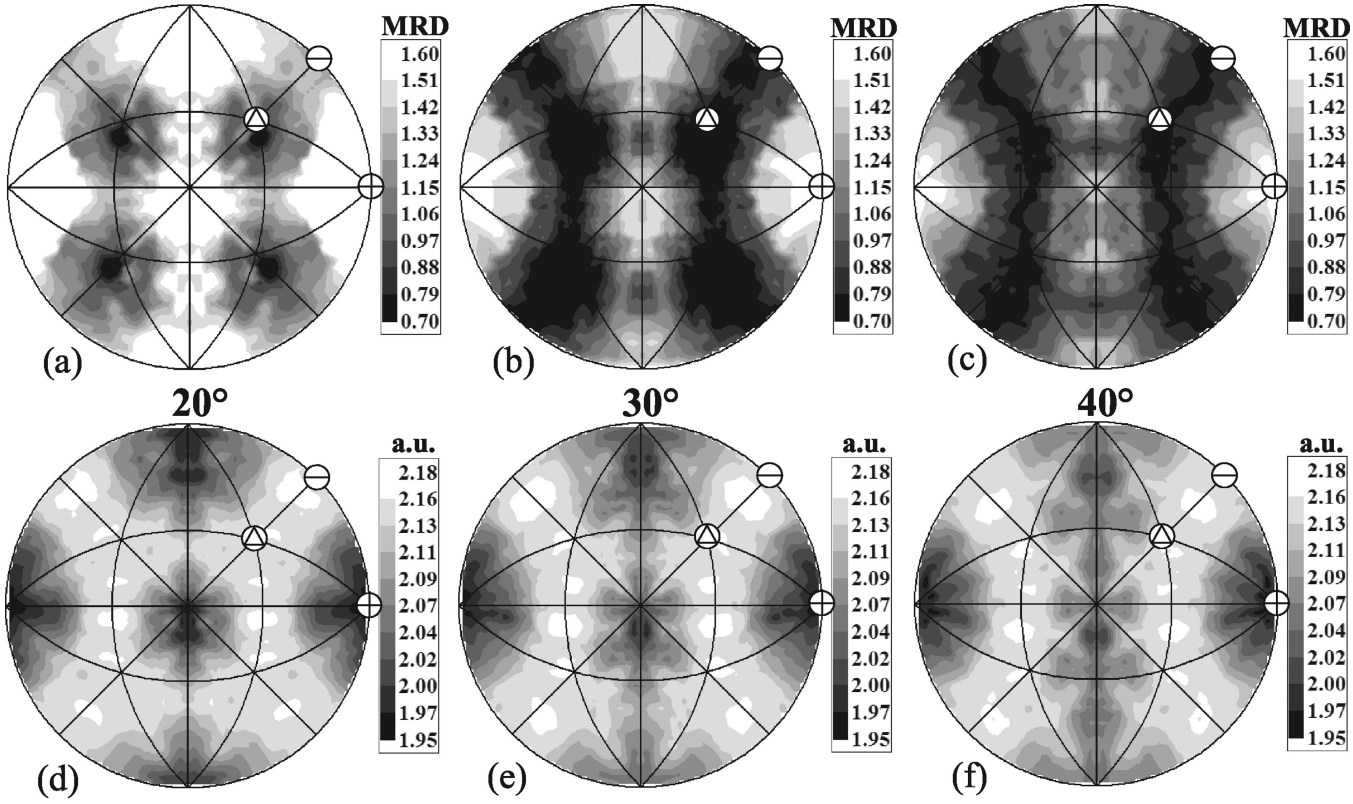

Fig. 6. Observed distribution of grain boundary plane normals for boundaries with misorientations of (a) 20°, (b) 30°, and (c) 40° around the [100] axis. The misorientation axis lies horizontally in the plane of the paper at the position of the [100] pole (indicated by the +). For comparison, the hypothetical grain boundary energies based on the sum of the two surface energies (d–f) at the same fixed misorientations are also shown.

are consistent with this idea and, in fact, are very similar to those reported previously for MgO. The lowest-energy surface of both $SrTiO_3$ and MgO is (100) and, in both cases, grain boundaries strongly favor these interface planes. Furthermore, in both cases, the population shows an inverse correlation with hypothetical grain boundary energies constructed from the sum of the two surface energies. We propose that two physical phenomena are responsible for this correlation. The first is the amplification of the low-energy boundary population at the expense of the high-energy boundaries by a combination of boundary repositioning and annihilation events that occur as an essential part of grain growth. The second phenomenon is the approximate constancy of the binding energy, which is the difference between the work to create two free surfaces and the work to create a grain boundary. As long as this binding energy is approximately constant, the surface energy anisotropy can be used to estimate the grain boundary energy anisotropy. Each of these phenomena is discussed separately in the following sections.

(1) Origin of the Textured Distribution

It seems reasonable to assume that the enhanced population of boundaries terminated by {100} planes is the result of their properties. The link between five-parameter grain boundary anisotropy and final-state microstructure in three-dimensional materials has not yet been explored in any detail. However, we have previously observed an inverse correlation between population and energy of boundaries in MgO[9] and the results from two-dimensional simulations provide some mechanistic guidance.[10,11] Holm *et al.*[10] used two-dimensional simulations to show that during grain growth, the population of grain boundaries with relatively a low energy increases and the population of high-energy boundaries decreases. During the simulation, the boundary distribution rapidly reaches a steady state and this state is not influenced by the anisotropy of the boundary mobility. Similar phenomena were reported by Upmanyu *et al.*,[12] who also argued that grain boundary energy is the dominant anisotropy in two-dimensional systems. These results were best explained by a model that increases the length of low-energy boundaries and reduces the length of high-energy boundaries to satisfy the interfacial equilibrium requirement at the triple points. We refer to this as the equilibrium boundary repositioning process. Note that this process does not affect the number density of the different types of boundaries; it simply makes low-energy boundaries longer and high-energy boundaries shorter. This prediction can be tested.

While the results presented here are per unit area, it is also possible to examine the number density of the boundaries. In other words, the boundaries can be counted by type, without normalizing by the area of each particular segment. To count the number density, we define a single "boundary" as a group of adjacent triangular segments that have the same misorientation and whose normals differ by less than 10°. When analyzed in this way, we find that the number density of boundaries is less anisotropic than the area normalized distribution; this indicates that the most commonly observed boundaries have larger average areas, as predicted by the model for the equilibrium boundary repositioning process. However, the remaining anisotropy is significant (approximately 2/3 of the total). In other words, not only are low-energy boundaries larger on average than high-energy boundaries, but there are more of them.

The increased number density of low-energy boundaries suggests that there is at least one additional mechanism at work. One possibility is that the grain boundary energy and mobility are related, so that higher-energy boundaries have higher velocities. If so, the faster boundaries move through neighboring grains at a higher rate and undergo more frequent annihilation. This can lead to an enhancement in the population of low-energy boundaries with respect to higher-energy boundaries. It should be noted, however, that since it is curved boundaries that migrate and such boundaries have a range of grain boundary normals, this mechanism can probably only apply to misorientation texture. For example, this might explain the observed enhancement in the population of low-misorientation-angle grain boundaries. In ongoing studies, we are attempting to determine the magnitude of the mobility anisotropy and the topological constraints that are needed to reproduce the observed anisotropies.

(2) Surface Energy–Grain Boundary Energy Correlation

The approximate constancy of the binding energy with grain boundary type means that relative surface energies can be used as reliable predictors of the relative grain boundary energy. If this is true, then the four parameters describing the two surface unit normals would be enough to specify the grain boundary energy. In other words, the grain boundary energy would be a function of four, not five, parameters. The fifth parameter (twist or rotation about the boundary normal) will not affect the energy. The population of boundaries should, therefore, also be independent of the twist angle and this is a supposition that we can test. The data in Fig. 7 illustrate the population of boundaries with [952] and [111] misorientation axes, as a function of twist angle. The upper curve shows that the population of general boundaries is, as supposed, independent of twist angle. However, the population does increase significantly at low misorientation angles (labeled $\Sigma 1$). This is expected, since it is known that the energies of low-angle boundaries decrease with misorientation angle. These boundaries are best thought of as being made up of coherent regions of crystal separated by dislocations. As the misorientation angle decreases and the amount of coherency increases, the binding energy is expected to increase and eliminate the influence of the surface energy on the grain boundary energy.

The populations for rotations about [111] are also shown in Fig. 7. These boundaries have the symmetry of their common triad axis so that the distribution is periodic with a 120° twist rotation and the special $\Sigma 3$ orientation relationships occurs at 60° and 180°. This boundary has the maximium possible planar coherency, with every boundary atom in a coincident position. As was the case for the low-angle grain boundary, it is not surprising that with such a remarkable degree of coincidence, the binding energy is significantly increased and the influence of the surface energies on the total interface energy is greatly reduced.

(3) Boundaries with low Σ CSL Misorientations

The enhanced population of $\Sigma 1$ and $\Sigma 3$ boundaries suggests that we should examine other boundaries that have a high planar coincident site density. The distributions of grain boundary planes at the four lowest Σ CSL misorientations are illustrated in Fig. 8. As mentioned earlier, the sample has no significant misorientation texture and the population of these particular misorientations is not significantly greater than any other. Of course, it must be understood that the misorientation itself does not guarantee high coincidence in the boundary plane. The interfaces of highest planar coincident site density are always the pure twist boundary (plane normal and misorientation axis parallel) and the symmetric tilt boundaries (when the misorientation axis is in the boundary plane and the surfaces on either side of the boundary are the same). For

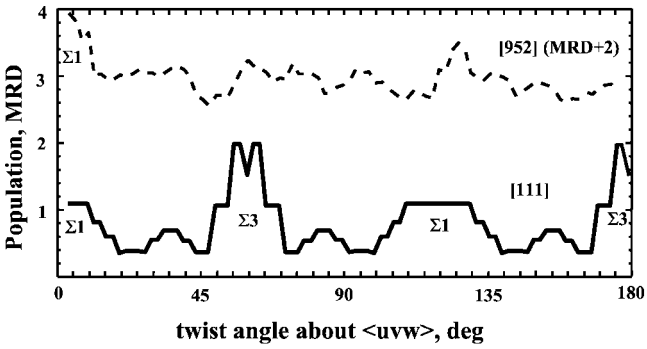

Fig. 7. Population of [111] and [952] twist boundaries as a function of the twist angle. The [952] data are offset by +2 MRD for clarity.

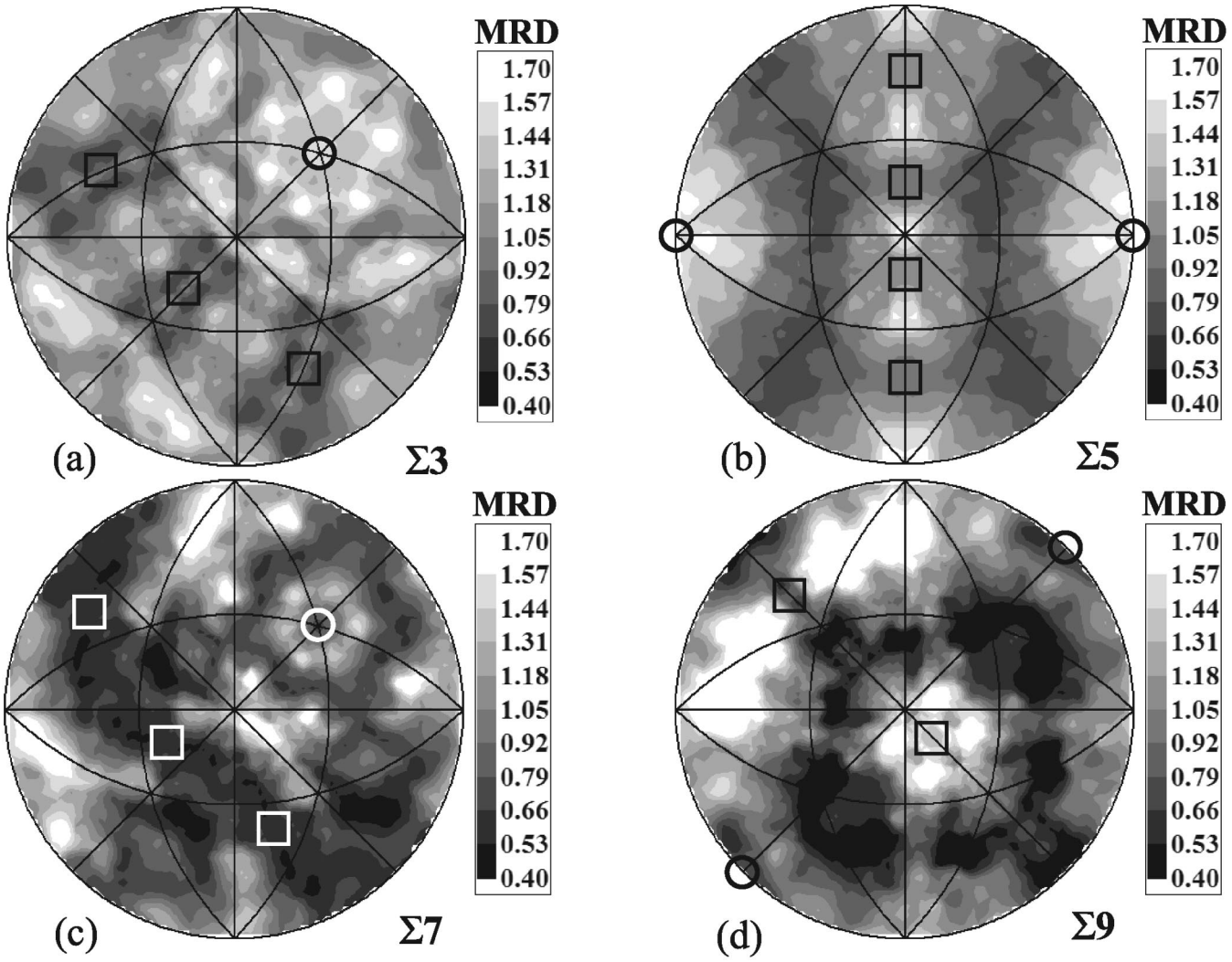

Fig. 8. Observed grain boundary plane normal distributions for (a) Σ3 (60°/[111]), (b) Σ5 (37°/[100]), (c) Σ7 (38°/[111]), and (d) Σ9 (39°/[110]) misorientations. In each plot, the squares mark the position of the symmetric tilts and the circles the positions of the pure twist boundaries: (a) twist $(\bar{1}\bar{1}\bar{1})$, tilt $(\bar{2}11)$, $(1\bar{1}\bar{2})$, and $(12\bar{1})$; (b) twist (100) and $(\bar{1}00)$, tilt (031), $(01\bar{2})$, $(0\bar{1}3)$, and $(02\bar{1})$; (c) twist (111), tilt $(\bar{3}21)$, $(\bar{2}\bar{1}3)$, and $(1\bar{3}2)$; (d) twist (110) and $(\bar{1}\bar{1}0)$, tilt $(\bar{2}\bar{2}1)$ and $(1\bar{1}4)$. The reference frame is the same as in Figs. 5 and 6.

the Σ3, we see a maximum in the vicinity of the pure twist boundary formed by two (111) planes rotated by 60°. This boundary, also referred to as a coherent twin, is the same one that created the peaks at 60° and 180° for [111] twist misorientations in Fig. 7. This is also the only example where a boundary formed by the highest-energy surface planes is a local maximum in the population. As mentioned before, this probably results from the coherency across this special boundary. Note that minima are found at the positions of the {211}-type symmetric tilt boundaries, which also have a high degree of planar coincidence.

The Σ5, Σ7, and Σ9 boundaries, on the other hand, are no different from the nonspecial points in misorientation space. The peaks are all correlated with boundaries that have planes near {100} and the complements to these surfaces; there are no distinct maxima at the planes of high coincidence. One apparent exception is the (100)‖(100) twist boundary at the Σ5 position. However, this maximum occurs at all [100] misorientations and is better explained by the presence of the two low-energy planes than by the coincidence condition. In the interpretation of these data, it should be noted that because misorientation space has been discretized in approximately 10° increments, the plots in Fig. 8 average the distribution of grain boundary planes at each CSL misorientation with those of neighboring misorientations within a 10° window. Thus, if there are cusps in the distribution at the CSL misorientations, the true population will be diluted by the coarse discretization. The effect is that extreme values move closer to the average value of 1. Thus, while the discretization may cause us to underestimate the actual values at the extreme positions in the distribution, it does not alter the basic conclusion that for misorientations other than Σ1 and Σ3, the coherent boundary planes that do not have the {100} orientation are local minima in the population.

Two points should be emphasized about the special nature of the Σ3 orientation relationship. The first is that the data in Figs. 7 and 8 show that the orientation relationship is significant only when the boundary is terminated by two (111) planes. Only this one configuration should be regarded as "special" by virtue of its relatively high population. The second point is that this boundary represents a very small fraction of the entire population, and its population is no higher than the {100} terminated boundaries that occur at all misorientations. For example, the {100} terminated boundaries in Figs. 5 and 6 all have populations greater than or equal to that of the coherent twin. The conclusion from this analysis it that while there are certain special boundaries such as Σ1 and Σ3 where there is a very high planar coincidence, the binding energy appears to be constant for the general boundaries and these are the interfaces that dominate the overall population.

Ernst *et al.*[12] have recently reported that the Σ3 orientation relationship occurs with a higher than random frequency in $SrTiO_3$. Using orientation imaging microscopy, 90 grain boundary misorientations were analyzed and 5 (6%) were found to have the Σ3 orientation relationship, within Brandon's[13] criterion. The

boundary plane orientations were not measured. When we analyze our data in the same way as Ernst *et al.*,[12] we find that of 75,088 20-μm grain boundary segments, 1276 have the Σ3 orientation relationship. This is 1.7% of the population and the calculated MRD value is 0.96. When we consider the fractional area, we find that 2.07% of the boundary plane area is within the same tolerance of Σ3 (corresponding to 1.18 MRD). In other words, boundaries with the Σ3 misorientation in our sample occur with the frequency expected in a random distribution. The enhanced population of Σ3 boundaries reported in the prior study might be the result of the sample composition (which contained 1 mol% excess TiO_2 and 0.4 atom% Fe doping).

One aspect of the tendency to form boundaries on {100} planes is that asymmetric configurations will naturally result. This is best seen along the axis of tilts in Fig. 8(b), where the peaks in the population are at (010)‖(043) and the minima are at the symmetric (012)‖(021) position. This observation is consistent with a recent study of the temperature dependence of the structure of a Σ5 tilt boundary in $SrTiO_3$, which found that an initially symmetric (310) boundary faceted into a configuration with parallel {100} and {430} planes when annealed in the range of 1100° to 1300°C.[14] These results suggest that below 1300°C, where the boundary facets, the population of symmetric boundaries falls to zero while the peaks at boundaries with {100}‖{043} configurations increase further. However, the present experiment was conducted at a temperature where the symmetric boundary was stable. In contrast to bicrystal experiments, where the macroscopic interface plane is constrained, the present experiment is sensitive to the entire range of boundary orientations. Hence, we observed both the stable symmetric interface as well as the more populous asymmetric configuration.

(4) Final Remarks

While the relationship between the surface energy anisotropy and the grain boundary energy anisotropy is a potentially useful simplifying principle, defining the ranges of conditions where it applies will require further research. For example, in materials with very little surface energy anisotropy, such as close-packed metals, variations in the binding energy that result from planar coincidence in the boundary are likely to dominate the grain boundary energy anisotropy. However, some support for the surface energy hypothesis can be found in the literature. For example, it has been noted that the grain boundary planes in a number of minerals are frequently orientated in low-index (and presumably low-energy) orientations.[15,16] Even in metals, where the surface energy is much more isotropic, past studies have noted the anisotropy of grain boundary planes and the tendency to facet on low-index planes.[17,18]

V. Summary

The grain boundary population in $SrTiO_3$ is correlated to the sum of the energies of the surfaces comprising the boundary. More boundaries are terminated by low-energy {100} planes than any other orientation. These observations suggest that the grain boundary energy is correlated to the surface energies of the planes on either side of the boundary and that the binding energy between the two surfaces is approximately constant. Two exceptions were identified: low-angle boundaries and the coherent twin where the boundary is comprised of two (111) planes rotated by 60°. In these special cases, it is assumed that the high degree of planar coincidence at the interface results in a significant increase in the binding energy.

References

[1]D. M. Saylor, A. Morawiec, B. L. Adams, and G. S. Rohrer, "Misorientation Dependence of the Grain Boundary Energy in Magnesia," *Interface Sci.*, **8** [2/3] 131–40 (2000).

[2]D. M. Saylor, A. Morawiec, and G. S. Rohrer, "Distribution and Energies of Grain Boundaries as a Function of Five Degrees of Freedom," *J. Am. Ceram. Soc.*, **85** [12] 3081–83 (2002).

[3]D. Wolf, "Correlation Between Structure, Energy, and Ideal Cleavage Fracture for Symmetrical Grain Boundaries in fcc Metals," *J. Mater. Res.*, **5** [8] 1708–30 (1990).

[4]D. M. Saylor, A. Morawiec, and G. S. Rohrer, "Distribution of Grain Boundaries in Magnesia as a Function of Five Macroscopic Parameters," *Acta Mater.*, **51** [13] 3663–74 (2003).

[5]T. Sano, D. M. Saylor, and G. S. Rohrer, "Surface Energy Anisotropy of $SrTiO_3$ at 1400°C in Air," *J. Am. Ceram. Soc.*, **86** [11] 1933–39 (2003).

[6]The naming of commercial equipment does not imply endorsement by NIST.

[7]W. H. Press, B. P. Flannery, S. A. Teukolsky, and W. T. Vetterling, *Numerical Recipes in Pascal.* Cambridge University Press, Cambridge, U.K., 1989.

[8]F. Williams, *Reasoning with Statistics.* Harcourt Brace Jovanovich, Fort Worth, TX, 1992.

[9]D. M. Saylor, A. Morawiec, and G. S. Rohrer, "The Relative Free Energies of Grain boundaries in Magnesia as a Function of Five Macroscopic Parameters," *Acta Mater.*, **51** [13] 3675–86 (2003).

[10]E. A. Holm, G. N. Hassold, and M. A. Miodownik, "On Misorientation Distribution Evolution During Anisotropic Grain Growth," *Acta Mater.*, **49** [15] 2981–91 (2001).

[11]M. Upmanyu, G. N. Hassold, A Kazaryan, E. A. Holm, Y. Wang, B. Patton, and D. J. Srolovitz, "Boundary Mobility and Energy Anisotropy Effects on Microstructural Evolution During Grain Growth," *Interface Sci.*, **10** [2–3] 201–16 (2002).

[12]F. Ernst, M. L. Mulvihill, O. Kienzle, and M. Rühle, "Preferred Grain Orientation Relationships in Sintered Perovskite Ceramics," *J. Am. Ceram. Soc.*, **84** [8] 1885–90 (2001).

[13]D. G. Brandon, "The Structure of High-Angle Grain Boundaries," *Acta Metall.*, **14** [11] 1479–84 (1966).

[14]S. B. Lee, W. Sigle, W. Kurtz, and M. Rühle, "Temperature Dependence of Faceting in the Σ5(310)[001] Grain Boundary of $SrTiO_3$," *Acta Mater.*, **51** [4] 975–81 (2003).

[15]R. Kretz, "Interpretations of Mineral Grains in Metamorphic Rocks," *J. Petrol.*, **7** [1] 68–94 (1966).

[16]D. Laporte and A. Provost, "Equilibrium Geometry of a Fluid Phase in a Polycrystalline Aggregate with Anisotropic Surface Energies: Dry Grain Boundaries," *J. Geophys. Res.*, **105** [B11] 25937–53 (2000).

[17]P. J. Goodhew, T. Y. Tan, and R. W. Balluffi, "Low Energy Planes for Tilt Grain Boundaries in Gold," *Acta Metall.*, **35** [4] 557–67 (1978).

[18]H. Ichinose and Y. Ishida, "Observation of [110] Tilt Boundary Structures in Gold by High Resolution HVEM," *Philos. Mag. A*, **43** [5] 1253–64 (1981). □